

Structural Basis for Asymmetric Association of the β PIX Coiled Coil and Shank PDZ

Young Jun Im^{1*}†, Gil Bu Kang²†, Jun Hyuck Lee²,
Kyoung Ryoung Park², Hye Eun Song², Eunjoon Kim³,
Woo Keun Song², Dongeun Park⁴ and Soo Hyun Eom^{2*}

¹College of Pharmacy, Chonnam National University, Gwangju 500-757, South Korea

²Department of Life Science, Cell Dynamics Research Center, Gwangju Institute of Science and Technology, Gwangju 500-712, South Korea

³Department of Biological Sciences, Korea Advanced Institute of Science and Technology, Guseong-dong, Daejeon 305-701, South Korea

⁴School of Biological Sciences, Seoul National University, Seoul 151-742, South Korea

Received 20 December 2009;
received in revised form
19 January 2010;
accepted 21 January 2010
Available online
29 January 2010

β PIX (p21-activated kinase interacting exchange factor) and Shank/ProSAP protein form a complex acting as a protein scaffold that integrates signaling pathways and regulates postsynaptic structure. Complex formation is mediated by the C-terminal PDZ binding motif of β PIX and the Shank PDZ domain. The coiled-coil (CC) domain upstream of the PDZ binding motif allows multimerization of β PIX, which is important for its physiological functions. We have solved the crystal structure of the β PIX CC–Shank PDZ complex and determined the stoichiometry of complex formation. The β PIX CC forms a 76-Å-long parallel CC trimer. Despite the fact that the β PIX CC exposes three PDZ binding motifs in the C-termini, the β PIX trimer associates with a single Shank PDZ. One of the C-terminal ends of the CC forms an extensive β -sheet interaction with the Shank PDZ, while the other two ends are not involved in ligand binding and form random coils. The two C-terminal ends of β PIX have significantly lower affinity than the first PDZ binding motif due to the steric hindrance in the C-terminal tails, which results in binding of a single PDZ domain to the β PIX trimer. The structure shows canonical class I PDZ binding with a β -sheet interaction extending to position -6 of β PIX. The β B– β C loop of Shank PDZ undergoes a conformational change upon ligand binding to form the β -sheet interaction and to accommodate the bulky side chain of Trp -5 . This structural study provides a clear picture of the molecular recognition of the PDZ ligand and the asymmetric association of β PIX CC and Shank PDZ.

© 2010 Elsevier Ltd. All rights reserved.

Edited by I. Wilson

Keywords: Shank; β PIX; PDZ; coiled coil; multimerization

Introduction

PIX (p21-activated kinase interacting exchange factor) proteins belong to a group of guanine

nucleotide exchange factors used by Rho GTPase family members Rac1 and Cdc42. Rho family proteins are known to regulate the actin cytoskeleton and to be involved in the formation of various types of focal adhesion structures.¹ They have also been implicated in a variety of other biological processes, including activation of gene transcription, cell cycle progression, microtubule dynamics, and vesicular trafficking.² During these processes, PIX interacts with numerous signaling proteins through its different domains and mediates the effects of various extracellular signals. PIXs are encoded by two genes, α PIX and β PIX, whose products include multiple splice variants (designated as β 1PIX, β 2PIX, and β 3PIX).¹ Both α PIX and β PIX (β PIX is used for β 1PIX unless otherwise designated) display

*Corresponding authors. E-mail addresses:
youngjun.im@gmail.com; eom@gist.ac.kr.

† Y.J.I. and G.B.K. equally contributed to this work.

Abbreviations used: PIX, p21-activated kinase interacting exchange factor; CC, coiled coil; SH3, Src homology 3; GIT, G-protein-coupled receptor kinase interacting protein; PAK, p21-activated kinase; GKAP, guanylate-kinase-associated protein; MAD, multiple anomalous dispersion; NTA, nitrilotriacetic acid; LI, loop insertion.

similar domain structures, including an N-terminal Src homology 3 (SH3) domain and a central Dbl homology/pleckstrin homology domain. The central Dbl homology/pleckstrin homology module mediates the nucleotide exchange for Rac and Cdc42. The C-terminal portion of PIX interacts with the Spa2 homology domain of GITs (G-protein-coupled receptor kinase interacting proteins), and the PIX SH3 domain associates with a proline-rich sequence in PAK (p21-activated kinase), thereby forming a large GIT–PIX–PAK heteromolecular complex.³ α PIX is distinguished from most β PIX isoforms by the presence of a calponin homology domain.⁴ At their C-terminal ends, both α PIX and β 1PIX contain a coiled-coil (CC) domain, whereas the corresponding region of β 2PIX is serine rich. The multimerization by its CC domain is essential for the peripheral localization of β 1PIX and to form a large PIX–PAK heteromolecular complex.^{5,6} β PIX has a PDZ binding motif in its extreme C-terminus that promotes the synaptic localization of β PIX by associating with the PDZ domains of Shank and hScrib.^{7,8}

The Shank/ProSAP family of multidomain scaffolding proteins is involved in organizing synaptic protein complexes.⁹ Shank contains several protein interaction domains, including ankyrin repeats, an SH3 domain, a PDZ domain, a proline-rich region, and a sterile α -motif domain. The Shank PDZ interacts with the GKAP (guanylate-kinase-associated protein) family of synaptic scaffolding proteins, as well as with a number of membrane proteins, including glutamate and somatostatin receptors.¹⁰ The canonical PDZ domain contains ~90 amino acids and folds into a compact globular structure composed of a six-stranded β -sandwich flanked by two α -helices. It binds specifically to short peptides at the extreme C-terminus of target proteins and/or an internal sequence that adopts a β -finger structure.¹¹ Through interactions with their target proteins, PDZ domains are often involved in organizing signal transduction complexes, clustering membrane receptors, and maintaining cell polarities.¹²

Shank recruits β PIX and β PIX-associated PAK to synaptic sites by its PDZ domain and regulates postsynaptic structure.⁷ Recent structural studies revealed that β PIX forms a parallel trimer by its CC domain.¹³ Still, there is limited knowledge about the precise mode of β PIX CC association with Shank PDZ. Here, we report the crystal structure of the complex between Shank PDZ and the C-terminal CC domain of β PIX. We examined how the complex adopts an unusual asymmetric architecture in which the β PIX CC trimer binds one Shank PDZ by hydrodynamic and thermodynamic analysis. The PDZ ligands used for structural studies have so far been limited to short peptides that mimic the C-terminal ends of target proteins. The current structure includes a PDZ ligand extending 60 residues upstream from the C-terminus and reveals how the binding motif associates with PDZ in conjunction with the upstream CC structure.

Results

Overall structure of the β PIX CC–Shank PDZ complex

The rat β PIX CC and Shank PDZ were coexpressed in *Escherichia coli* using a bicistronic expression vector (Fig. 1a). The crystal structure of the complex was determined using SeMet multiple anomalous dispersion (MAD) at 2.8-Å resolution. The resultant $2F_o - F_c$ electron density map clearly shows the bound β PIX C-terminal residues in a binding pocket (Fig. 1b). The refined structure consists of three copies of β PIX (residues 587–646) in a triple CC and a single Shank PDZ domain bound to one of the C-termini of β PIX chains (Fig. 1c). As expected from the predicted secondary structure, the β PIX CC domain, which spans 52 residues (residues 587–638), forms a single α -helix, and the three copies of the CC domain form a parallel CC structure (Fig. 1d and e). The overall conformations of the three CC domains are similar, with a C $^\alpha$ rmsd of 1.2–1.7 Å for residues 589–634. The CC is 76 Å in length and contains seven heptad repeats (Leu590, Leu597, Leu604, Met611, Glu618, Leu625, and Val632) (Fig. 1f). Its structure is formed by hydrophobic residues at positions a and e of the heptad repeats, which is characteristic of CC structures.¹⁴ Thirty-three basic residues (11 basic and 5 acidic residues per subunit) are located in the C-terminal half of the CC, which gives it an overall positive electrostatic potential (Fig. 1g). β PIX is well conserved among mammals, with the rat homolog showing 94% identity to the human one. The amino acid sequences of the rat β PIX CC region (β PIX CC) and the Shank PDZ used in this study are identical with the human homologs. In addition, the amino acid residues contributing to CC formation are strictly conserved among PIX family members and the eight variable residues are all located on the surface of the structure, suggesting that the human α PIX and β 1PIX isoforms might form homo- or heterotrimers (Fig. 1f). The β PIX CC structure is terminated by Pro639, which is immediately followed by a PDZ binding motif (AWDETNL). Unexpectedly, the C-terminal residues of each subunit have completely different conformations (Fig. 1h). The seven C-terminal residues of chain A, which interacts with the Shank PDZ, form an extended β -strand structure, while the C-terminal residues of chains B and C form random coils. The C-terminus of chain B is exposed to the solvent and folds back toward the base of the CC, while the C-terminus of chain C (residues 638–646) is disordered and not visible in the electron density map. This conformational difference in the C-terminal ends of the β PIX subunits suggests that the flexible PDZ binding motif is disordered in its unbound state and undergoes conformational change to form a β -strand upon PDZ binding.

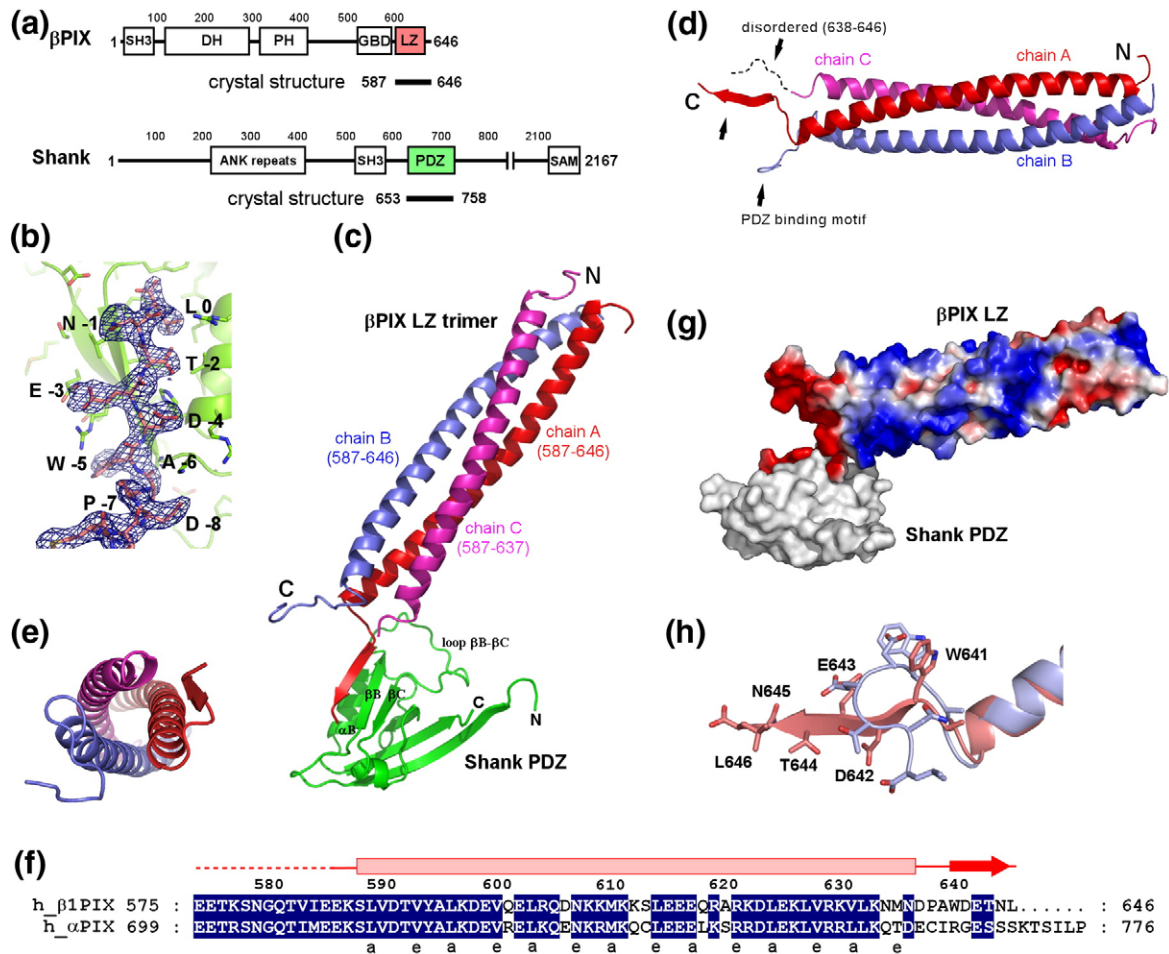


Fig. 1. Structure of the β PIX–Shank PDZ complex. (a) Schematic of constructs used for crystallography and the domain structures of β PIX and Shank proteins from *Rattus norvegicus* (Swiss-Prot accession number O55043 for β PIX; Swiss-Prot accession number Q9WV48 for Shank). The domains are drawn to scale, and the amino acid numbers are shown for each hundred residues. (b) The 2.8-Å $2F_o - F_c$ electron density map corresponding to the C-terminal PDZ binding motif of β PIX. The Shank PDZ is shown in ribbon representation, and the C-terminal residues of β PIX are shown in ball-and-stick representation. Residues are numbered 0 to –8 from the last residue at the C-terminus of β PIX. (c) Overall structure of the β PIX–Shank PDZ complex. The Shank PDZ domain is shown in green. Three β PIX CC helices are shown in red, blue, and magenta. (d) Ribbon representation of the β PIX CC trimer. (e) Bottom view of the β PIX CC trimer. (f) Sequence alignment of human α PIX and β PIX. Secondary structural elements are shown as bar and arrow. The heptad repeats of the CC are labeled ‘a’ and ‘e’. (g) Electrostatic surface representation of the β PIX CC domain. The surface of the Shank PDZ is shown in white. (h) Superposition of the C-terminal residues of chains A and B of β PIX.

Structural determinant for the binding of β PIX to the Shank PDZ

The Shank PDZ is a compact globular domain containing eight secondary structural elements. Six β -strands and two α -helices form a β -sandwich structure, and a 19-residue loop is inserted between β B and β C.¹⁵ The seven C-terminal residues of β PIX are positioned in a groove between strand β B and helix α B and are oriented as an additional strand anti-parallel with β B (Figs. 1c and 2a). The orientation of the C-terminal PDZ binding motif is parallel with the CC, and the PDZ domain is closely bound to the base of the CC structure (Fig. 1c). The three C-terminal residues (TNL) bind to the PDZ domain in a canonical class I PDZ interaction.¹¹ Leu 0, the first

residue, binds to the hydrophobic pocket, and Thr –2 makes a hydrogen bond with His735, which is a signature of the class I PDZ interaction [–(T/S)–X–L] (Fig. 2a). The side chain of Asn –1 is exposed to the solvent and does not interact with the PDZ domain. In addition, Glu –3 makes an electrostatic contact with the conserved Arg679, and the side chain of Trp –5 is positioned in the hydrophobic groove formed by Tyr701, Arg679, and Phe696 of the β B– β C loop (Fig. 2a and b). Finally, the side chains of Asp –4 and Asp –8 are oriented toward the basic patch formed by Lys682 and Arg736 at a distance of 3.6–4.5 Å, which appears to further stabilize the PDZ–ligand interaction.

To examine the PDZ–ligand interaction in more detail, we carried out Ni-NTA (nitrilotriacetic acid)

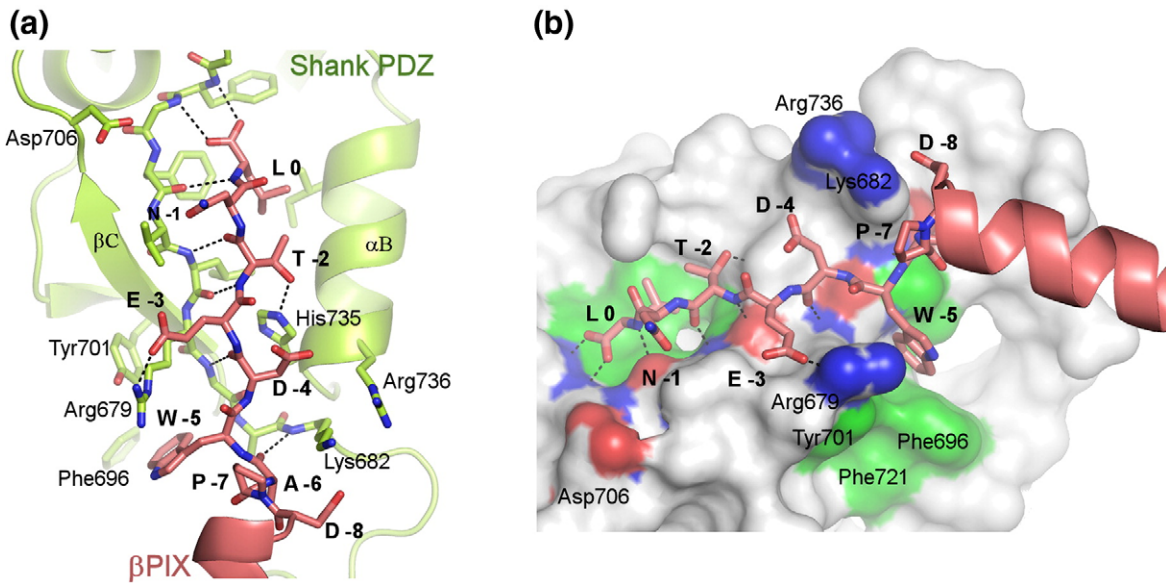


Fig. 2. Recognition of the β PIX C-terminal residues by the Shank PDZ. (a) Binding of the β PIX C-terminal residues to the Shank PDZ. The Shank PDZ is shown in light green; β PIX is in pink. Hydrogen bonds are shown as dashed lines. For clarity, chains B and C of β PIX are not shown. (b) Molecular surface representation of the peptide binding pocket in the Shank PDZ. The bound C-terminal residues of β PIX are shown in ball-and-stick representation, and the CC is shown in ribbon representation. Chains B and C of β PIX are not shown.

pull-down of β PIX mutant and His-tagged Shank PDZ from cell lysate (Fig. 3). Mutation of Trp -5 of β PIX to Ala significantly reduced PDZ binding, but alanine mutation of Glu -3 or Asp -4 had little effect. Mutation of the conserved Arg679 in the Shank PDZ to Ala completely abolished the ligand

binding. Arg679 interacts with residues -3 and -5 of β PIX: its guanidyl group makes an electrostatic contact with Glu -3, and the stalk of its side chain forms a wall of the hydrophobic pocket into which Trp -5 binds. This suggests that Glu -3 and Trp -5 act to increase ligand affinity and specificity by interacting with Arg679 in strand β B. Truncation of the β B- β C loop to 6 residues ($\Delta\beta$ B- β C loop) abolished the association with β PIX. This is consistent with the weak binding of the alanine mutant of Trp -5 in that the β B- β C loop provides a binding pocket for Trp -5. The deletion of 13 residues (587-599) at the N-terminus of the β PIX CC (construct 600-646) did not disrupt formation of the β PIX-Shank PDZ complex. To test whether the proximity of the CC domain and the PDZ binding motif is essential, we inserted a flexible loop with 15 residues between the CC domain and the PDZ binding motif (AWDETNL). The loop insertion (LI) mutants showed binding similar to the wild type, which confirms that the upstream of the 7 C-terminal residues is not directly involved in PDZ binding.

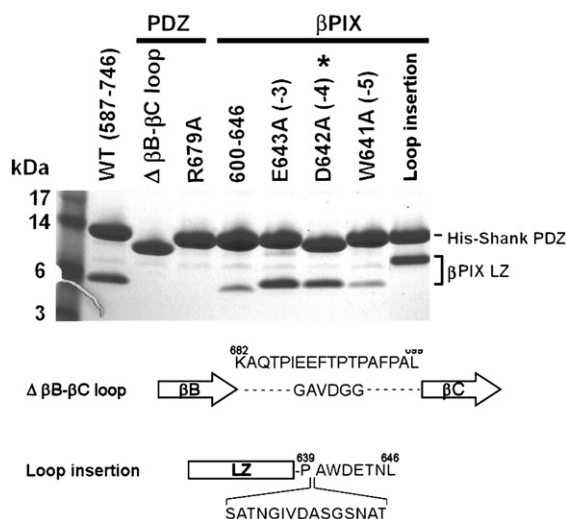


Fig. 3. Ni-NTA pull-down of various mutants. Various constructs of the β PIX CC and His-tagged Shank PDZ were coexpressed in *E. coli*, and the cell lysates were loaded onto Ni-NTA beads, after which samples of the eluate from the Ni-NTA beads were subjected to SDS-PAGE analysis. The coexpression of two proteins yielded higher levels of His-tagged Shank PDZ than β PIX CC. The asterisk indicates that the D642A mutant lacking the N-terminal thrombin cleavage sequence (LVPRGS) runs slightly faster in SDS-PAGE.

Conformational change in the Shank PDZ upon β PIX binding

Superposition of the β PIX-Shank PDZ complex and the apo PDZ domain [Protein Data Bank (PDB) ID 1Q30] reveals the ligand-induced conformational changes in the PDZ domain. The major change in the Shank PDZ structure occurs in the β B- β C loop (Fig. 4). This conformational change was not examined in a previous structural study of the Shank PDZ-GKAP peptide complex because the β B- β C loop was disordered by the lack of interaction with the short peptide.¹⁵ The long

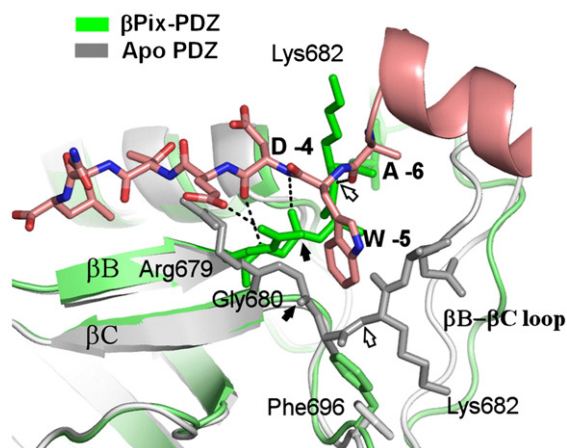


Fig. 4. Conformational change in the PDZ domain upon ligand binding. The Shank PDZ is shown in green; β PIX is in pink. The structure of the apo-PDZ (PDB ID 1Q30) is shown in gray. The filled black arrow and open arrow indicate the backbone oxygen atom of Gly680 and the backbone nitrogen atom of Lys682, respectively.

β B– β C loop (residues 683–698) is highly flexible; in fact, it has the highest *B*-factors in the structure, and three residues (687–689) were not well defined in the electron density map. Upon β PIX binding, the N-terminal part of loop β B– β C (residues 680–682) moves toward helix α B to accommodate the bulky hydrophobic Trp –5 residue of β PIX. The reorientation of the backbones of residues 680–682 creates a β -sheet interaction with the C-terminal residues of β PIX at positions –4, –5, and –6 (Fig. 4). This conformational change eliminates the clashes of Trp –5 with residues 680–682. Lys682 undergoes the largest conformational change, during which the C $^{\alpha}$ atom is displaced by 11 Å. The relocated Lys682 makes an electrostatic contact with Asp –8 of β PIX, and the side chain of Phe696 rotates toward Trp –5 to form a hydrophobic groove. This conformational change in loop β B– β C appears to be essential for ligand binding in that it provides a hydrogen-bonding partner and a hydrophobic pocket for the –4, –5, and –6 positions of the PDZ binding motif of β PIX.

Oligomeric association of the β PIX–Shank PDZ complex

β PIX and Shank PDZ form a complex with a 3:1 molar ratio in the crystal. The structure of the β PIX CC determined in this study is consistent with the recent structural studies that demonstrated that the C-terminal domain of β PIX forms a parallel CC trimer in crystal and in solution.¹³ The Shank PDZ domain binds to only one of the three β PIX CC chains and makes few interactions with the other two chains of the β PIX trimer. Coexpression of wild-type β PIX CC and Shank PDZ in *E. coli* produced a complex of a 3:1 molar ratio with excess free PDZ protein (Fig. 5a and b). We confirmed that the isolated Shank PDZ is a monomer in solution as

demonstrated by hydrodynamic analysis (Fig. 5c). The measured R_H value of free PDZ (2.1 nm) is consistent with the value derived from the structure of monomeric PDZ (2.0 nm). The experimental Stokes radius of the β PIX–Shank PDZ (3.2 nm) agreed with the calculated value (3.3 nm) from the structural coordinates of the 3:1 complex (Fig. 5c). The oligomeric species with a 3:3 or 3:2 molar ratio were not detected in wild-type constructs during purification. This observation raises a key question regarding the asymmetric association of a β PIX trimer and a Shank PDZ since the CC of β PIX has three identical C-termini for PDZ binding. The PDZ binding motifs begin right after the C-terminal ends of CC domains and all three C-termini are in close proximity to one another. This configuration might interfere with the binding of additional PDZ molecules to the 3:1 complex by steric hindrance. To prove this hypothesis, we inserted a flexible loop with 15 residues before the PDZ binding motif to provide spatial separation of the three binding motifs. The insertion mutants were then analyzed by size-exclusion chromatography and SDS-PAGE to measure the ratio of β PIX and PDZ molecules in the complexes (Fig. 5a and b). The insertion mutant showed a significant decrease of retention volume compared with the wild-type complex in size-exclusion chromatography. The shift of the peaks can be best explained by the incorporation of additional PDZ molecules to the complex. The densitometric analysis of Coomassie-stained protein bands corresponding to each peak demonstrates that the insertion mutants have a molar ratio close to 3:3. In order to confirm that the single PDZ association to β PIX trimer is caused by steric hindrance, we measured the binding affinity of Shank PDZ to β PIX trimer by isothermal titration calorimetry (Fig. 5d). The binding curve could not be fit to a single-binding-site model. Instead, the curve was best fit to a two-binding-site model with a strong binding site ($K_{d1}=2.6 \mu\text{M}$) and a weak binding site ($K_{d2}=16.3 \mu\text{M}$). We could not measure the accurate stoichiometry because the protein solubility could not be reached to measure the full curve of strong and weak binding sites. This result can be comprehended such that the second binding sites are influenced by the PDZ binding to the first site by steric hindrance. Therefore, the spatial separation by the insertion of a linker would fully expose the three C-terminal ends for independent PDZ bindings. As expected, insertion of a 15-residue loop between the CC and the PDZ binding motif showed a single binding curve ($K_d=9 \mu\text{M}$) with a stoichiometry of 3 (Fig. 5e), suggesting that the three C-terminal ends of mutant β PIX are fully exposed for PDZ binding and form a 3:3 complex with Shank PDZ. These data confirm that the crowding of the C-terminal PDZ binding motifs by oligomerization of the CC domain leads to reduced binding of the second and third binding motifs by steric hindrance, which explains the formation of the asymmetric 3:1 β PIX–Shank PDZ complex.

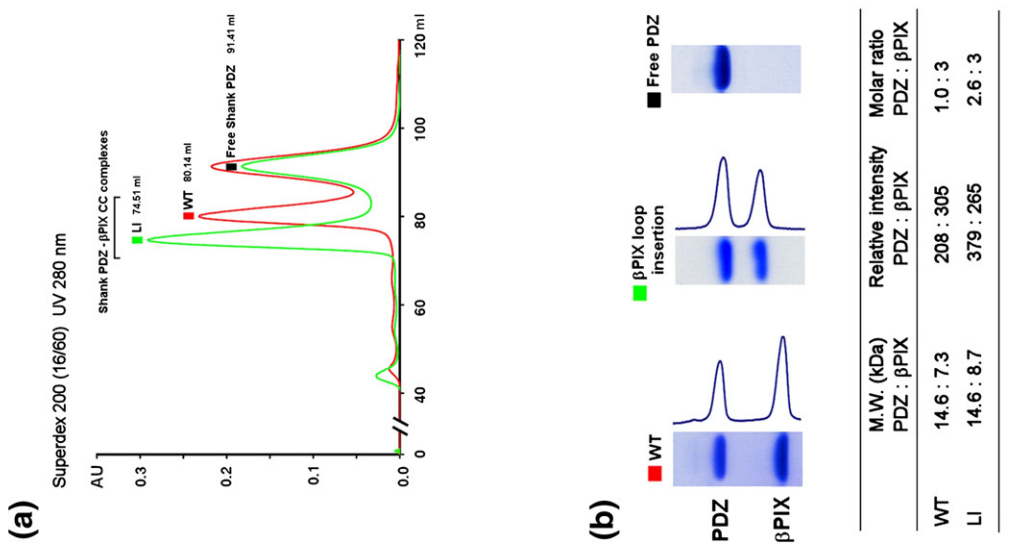
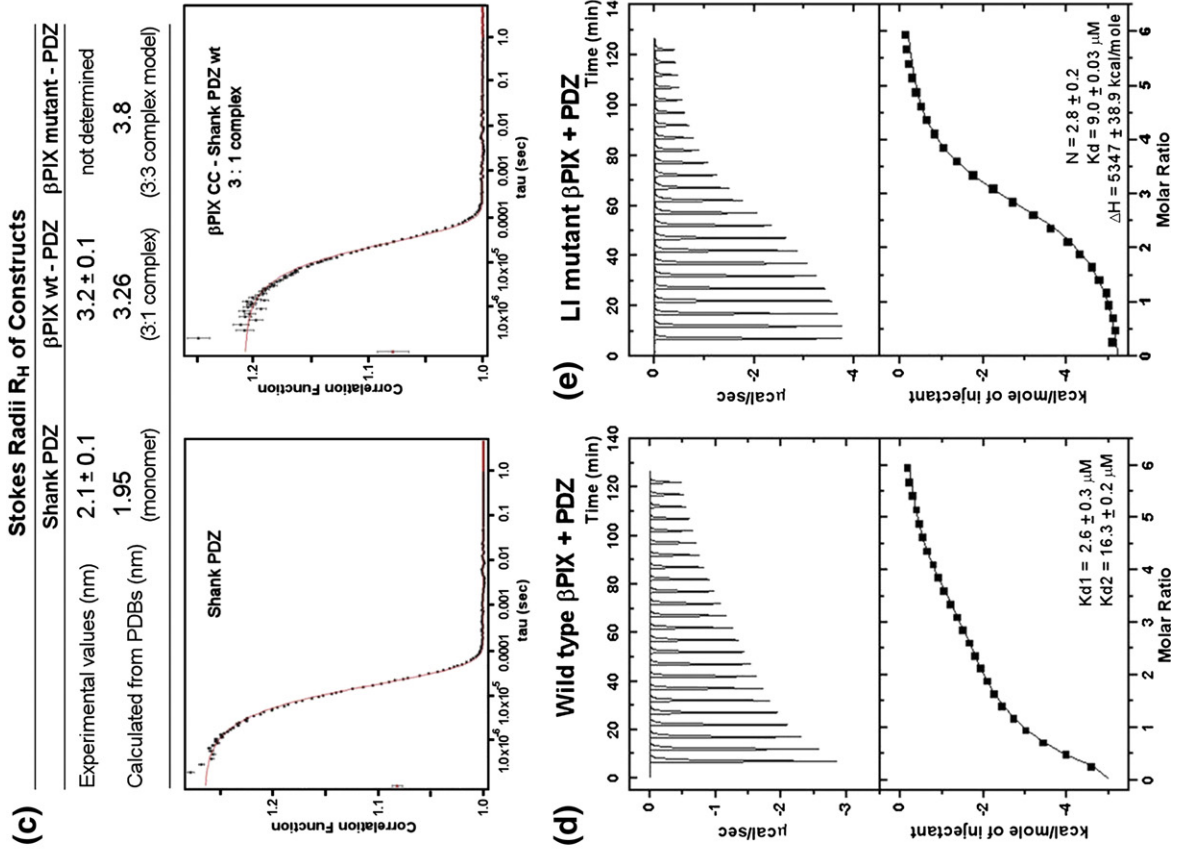


Fig. 5 (legend on next page)

Discussion

The mode of β PIX CC–Shank PDZ binding is consistent with the canonical class I PDZ interaction. The side chains of Leu 0, Thr –2, Glu –3, and Trp –5 directly interact with the Shank PDZ, and the affinity is enhanced by auxiliary interactions with the residues upstream of the core motif (TNL) of β PIX. Recognition of the residue at position –5 is mediated by the β B– β C loop and Arg679. The Shank PDZ accompanies a conformational change in the β B– β C loop upon β PIX binding. Notably, the β B– β C loop varies greatly with respect to sequence, length, and main-chain conformation among different PDZ domains, which suggests that the β B– β C loop may serve as an additional determinant of ligand specificity and affinity.¹⁶ Previously, we proposed a model of a dimeric Shank PDZ– β PIX complex based on the artifactual PDZ dimer observed in the crystal lattice.¹⁵ In this study, we confirmed that Shank PDZ is a monomer in solution by dynamic light scattering analysis. We found that the β PIX CC domain is a CC trimer and that β PIX and Shank PDZ form a 3:1 complex. The trimeric CC structure is consistent with a recent structural study on β PIX CC domain with an rmsd of 0.8 Å.¹³ The full-length Shank has multiple domains on either side of the N- and C-termini of the PDZ domain, and the β PIX trimer has three C-terminal PDZ binding motifs close to one another. Therefore, the β PIX trimer *in vivo* would associate with one Shank molecule due to the reduced affinities of the second and third PDZ binding motifs by steric hindrance. The PDZ binding motif is present only in the β 1PIX isoform; therefore, the hetero-oligomers of PIX isoforms would have an asymmetric association with PDZ, similar to the β PIX–Shank PDZ complex seen in this crystal structure. Since the binding of one Shank molecule is sufficient to recruit the β PIX, the 3:1 association of β PIX CC and Shank PDZ would be physiologically relevant. Asymmetric association of β PIX is not limited to Shank protein. β PIX and GIT1 are known to form homo-oligomers by their CC domains, and they also form an asymmetric heteropentameric complex consisting of a PIX trimer and a GIT1 dimer.^{5,13,17,18} GIT and PIX proteins are tightly associated as a multimeric complex capable of linking important signaling

molecules, including PAKs.^{3,18} PIX and GITs colocalize at focal complexes, the cell periphery, and cytoplasmic complexes.^{19,20} Oligomerization by the CC domains appears to be essential for specific subcellular localizations since mutations that disrupt PIX oligomerization cause it to be diffusely distributed in the cytoplasm.^{5,17,19} We did not detect membrane binding of the C-terminal CC region of β PIX using liposomes composed of phosphatidylcholine, phosphatidylethanolamine, and phosphoinositides *in vitro* (data not shown). The localization of β PIX seems to be mediated by the C-terminal PDZ binding motif downstream of the CC region because Shank associates with β PIX via its PDZ domain and recruits β PIX and PAK to synaptic sites.⁷ The PDZ domain of hScrib scaffolding protein also directly binds to β PIX, which is required to anchor β PIX at the cell cortex.⁸ It thus appears that hScrib and Shank act as membrane anchors for β PIX, which can then recruit GIT and other associated proteins. In summary, our structural studies provide a clear picture of the asymmetric association of β PIX and Shank PDZ, which is the basis for β PIX recruitment to synaptic sites.

Material and Methods

Protein expression and purification

DNA encoding the rat Shank PDZ (residues 653–763) was subcloned into the BamHI and HindIII sites of a pETDuet-1 vector modified to contain an N-terminal hexahistidine tag separated from the protein by a thrombin protease recognition site. The DNA encoding β PIX (residues 586–646) was subcloned into the second multiple cloning site of the modified pET-Duet vector using NdeI and XhoI (GenBank accession number NM_001113521.1 for β PIX; GenBank accession number NM_031751 for Shank). The β PIX–Shank PDZ complex was expressed in *E. coli* BL21(DE3) at 30 °C. The cell lysate was applied to a Ni-NTA affinity column. After washing the column with lysis buffer (200 mM NaCl and 50 mM NaH₂PO₄, pH 7.5), we eluted the complex using buffer (250 mM imidazole, 200 mM NaCl, and 50 mM NaH₂PO₄, pH 7.5). The eluate was concentrated to 15 mg/ml, and the histidine tag in the Shank PDZ was removed with thrombin protease. The protein complex was further purified by a Superdex 200 size-exclusion column (Pharmacia) equilibrated with buffer containing 20 mM Tris–

Fig. 5. Oligomeric states of the β PIX–Shank PDZ complex. (a) Size-exclusion chromatography profiles of the β PIX–Shank PDZ constructs after Ni-NTA affinity purification. Red and green indicate wild type and the LI (loop insertion) mutant, respectively. The coexpression of two proteins in *E. coli* yielded higher levels of His-tagged Shank PDZ than β PIX CC, resulting in a mixture of the complex and the excess free Shank PDZ. In each profile, the first peak corresponds to the β PIX–Shank PDZ complex and the second peak corresponds to free Shank PDZ. (b) The SDS-PAGE of each peak from size-exclusion chromatography and the results of the densitometric analysis are shown. The molar ratio of β PIX CC and Shank PDZ was measured by analyzing the amount of each protein from a scanned image using the program LabWorks. (c) Hydrodynamic analysis of the β PIX–Shank PDZ complex. The table shows the experimental and calculated R_H values. The experimental Stokes radii R_H were measured by dynamic light scattering. The calculated R_H values were derived from the crystal structures of the Shank PDZ and the β PIX–Shank PDZ complex. The R_H value of β PIX mutant–Shank PDZ could not be measured due to the partial dissociation of PDZ from the complex upon isolation. The calculated R_H value was derived from a structural model of the 3:3 complex. The lower panels show the correlation curves of the dynamic light scattering data. (d) Isothermal titration calorimetry of Shank PDZ into wild-type β PIX CC solution. (e) Isothermal titration calorimetry of Shank PDZ into mutant (linker insertion) β PIX CC solution.

Table 1. Data collection and refinement statistics

Crystal	Native		SeMet derivative	
Space group	$P3_212$		$P3_212$	
Cell dimensions (Å)				
<i>a</i>	47.7		48.0	
<i>b</i>	47.7		48.0	
<i>c</i>	263.2		262.5	
X-ray source	PAL 4A		PF BL5	
Wavelength (Å)	0.9199		Inflection, 0.9796	Peak, 0.9795
Resolution (Å) (last shell)	2.8 (2.8–2.9)		3.1 (3.1–3.15)	3.1 (3.1–3.15)
No. of unique reflections	8492		6605	6632
<i>I</i> / σ	36.6 (4.2)		63.7 (8.8)	63.5 (8.4)
Redundancy	4.8		12.7	13.1
R_{sym} (%) ^a	5.4 (36.1)		6.7 (28.9)	7.6 (29.9)
Data completeness (%) ^a	95.6 (93.4)		99.5 (98.2)	99.6 (98.1)
<i>Phasing and refinement statistics</i>				
Mean figure of merit (50–3.1 Å)			0.63 (SOLVE)	
Overall figure of merit (50–3.1 Å)			0.74 (RESOLVE)	
No. of reflections used	8092			
<i>R</i> -factor (%)	27.2 (43.4)			
Free <i>R</i> -factor (%) ^b	30.7 (49.2)			
rms bond length (Å)	0.007			
rms bond angle (°)	1.3			
No. of atoms				
Protein	2291			
Water	20			
Average <i>B</i> -value (Å ²) ^c	91.1 (Wilson <i>B</i> -factor of data set, 103.8)			
Ramachandran plot (%)				
Favored and allowed regions	94.5			
Generously allowed regions	3.9			
Disallowed regions	1.6			

^a The values in parentheses relate to the highest-resolution shells.

^b R_{free} was calculated with 5% of the data.

^c Average *B*-value of all atoms in an asymmetric unit.

HCl, pH 8.0, and 100 mM NaCl. The fractions containing the recombinant protein were concentrated to 15 mg/ml. The SeMet-labeled protein was expressed in *E. coli* strain B834(DE3) in M9 minimal medium supplemented with selenomethionine and was purified using the same protocol used for the native protein complex.

Mutagenesis

The mutations were carried out with a QuikChange Site-Directed Mutagenesis Kit (Stratagene) using the modified pETDuet vector containing the β PIX CC and Shank PDZ genes as a template. The open-reading frames of all mutant genes were confirmed by DNA sequencing.

Hydrodynamic analysis

The experimental Stokes radii R_{H} of the proteins were measured using a Wyatt quasi-elastic light scattering instrument with ASTRA V software. The calculated R_{H} values of the β PIX–Shank PDZ complex and the free PDZ were derived from crystal structures using the program Hydropro.²¹

Isothermal titration calorimetry

The individual Shank PDZ, β PIX, and β PIX LI mutant were expressed in *E. coli* using the pGEX-4T–Shank PDZ, pHIS- β PIX, and pHIS- β PIX LI vectors, respectively. Shank PDZ was purified by glutathione affinity and size-exclusion chromatography. β PIX constructs with an N-terminal hexahistidine tag followed by a TEV cleavage

site were purified by Ni²⁺ affinity and size-exclusion chromatography. The N-terminal affinity tags were removed by protease cleavage during purification steps. Shank PDZ (2 mM, injectant), wild-type β PIX (75 μ M, placed in the sample cell), and the linker insertion mutant of β PIX (75 μ M, placed in the sample cell) were dissolved in 20 mM Tris–HCl, pH 8.0, and 40 mM NaCl. Titrations (25 injections of 12 μ l of Shank PDZ) were performed at 25 °C using a VP-ITC Microcalorimeter (MicroCal), and data were analyzed using Origin software (Origin Lab).

Crystallization

Single crystals of the β PIX–Shank PDZ complex were grown at 21 °C in 2- μ l hanging drops containing equal volumes of protein solution (15 mg/ml) and mother liquor [100 mM Mes–NaOH, pH 6.5, 15% (v/v) ethanol, and 10% (v/v) ethylene glycol]. The crystals grew to a maximum size of 0.1 mm \times 0.2 mm \times 1.0 mm over 1 week. The crystals were cryoprotected in reservoir solution supplemented with 20% ethylene glycol and flash frozen under N₂ gas at 95 K.

Crystallographic analysis

Native data were collected at 2.8-Å resolution from a single frozen crystal using an ADSC Quantum Q210 CCD detector at beamline 4A of the Pohang Accelerator Laboratory (South Korea). All data were processed and scaled using HKL2000 (HKL Research). In addition, MAD data sets were collected using SeMet-labeled crystals with an ADSC Quantum 315 CCD detector at beamline BL5 of

the Photon Factory (Japan). MAD phasing was carried out using the program SOLVE²² at 3.1-Å resolution (Table 1). SeMet crystals displayed significant radiation decay and weak anomalous signals. Therefore, the wedge data collection was essential to obtain good MAD phasing. Of 14 sites in the complex, 2 Se sites were found. The phases were further improved using RESOLVE²² and it showed clear electron densities for βPIX and Shank PDZ. Automatic model building was carried out using RESOLVE, with which about 50% of the structure was modeled. The structure of the Shank PDZ (PDB ID 1Q3O) was fit into the partially built model. The remainder of the model was then built manually into a density-modified map using the program O, and the structure was refined using CNS²³ and REFMAC with TLS refinement.²⁴ The model constructed from the MAD data was used as a starting model for the 2.8-Å native data. After rigid-body refinement and cycles of simulated annealing, a readily interpretable map was obtained, and the structure was further built and refined. The eight C-terminal residues (638–646) of one of the three βPIX subunits were disordered and were not modeled in the structure. The final model, which consisted of three copies of the βPIX CC, one Shank PDZ, and 20 water molecules, was refined at 2.8-Å resolution to an *R*-factor of 27.2% with a free *R*-value of 30.7%. The data set has a high Wilson *B*-value of 73.9 Å², and the model was refined to an average *B*-factor of 91.1 Å². The model had no residue in a disallowed region of the Ramachandran plot, except for four residues in the disordered loop regions.

Accession number

The atomic coordinates and structure factors have been deposited in the PDB (www.pdb.org) with the code 3L4F.

Acknowledgements

This work was supported by the Ministry of Education, Science, and Technology through grants R11-2007-007-03001-0, 20090065566, and R01-2007-000-10592-0 and the Gwangju Institute of Science and Technology through a “Systems Biology Infrastructure Establishment Grant.” We thank Tom Leonard, Daniel Kloer, and Thomas Wollert for comments on the manuscript and the staff at beamlines 4A and BL5 of the Pohang Accelerator Laboratory and the Photon Factory, respectively, for user support.

References

- Rosenberger, G. & Kutsche, K. (2006). alphaPIX and betaPIX and their role in focal adhesion formation. *Eur. J. Cell Biol.* **85**, 265–274.
- Etienne-Manneville, S. & Hall, A. (2002). Rho GTPases in cell biology. *Nature*, **420**, 629–635.
- Premont, R. T., Perry, S. J., Schmalzigaug, R., Roseman, J. T., Xing, Y. & Claing, A. (2004). The GIT/PIX complex: an oligomeric assembly of GIT family ARF GTPase-activating proteins and PIX family Rac1/Cdc42 guanine nucleotide exchange factors. *Cell. Signal.* **16**, 1001–1011.
- Rosenberger, G., Jantke, I., Gal, A. & Kutsche, K. (2003). Interaction of alphaPIX (ARHGEF6) with beta-parvin (PARVB) suggests an involvement of alphaPIX in integrin-mediated signaling. *Hum. Mol. Genet.* **12**, 155–167.
- Koh, C. G., Manser, E., Zhao, Z. S., Ng, C. P. & Lim, L. (2001). beta1PIX, the PAK-interacting exchange factor, requires localization via a coiled-coil region to promote microvillus-like structures and membrane ruffles. *J. Cell Sci.* **114**, 4239–4251.
- Za, L., Albertinazzi, C., Paris, S., Gagliani, M., Tacchetti, C. & de Curtis, I. (2006). betaPIX controls cell motility and neurite extension by regulating the distribution of GIT1. *J. Cell Sci.* **119**, 2654–2666.
- Park, E., Na, M., Choi, J., Kim, S., Lee, J. R., Yoon, J. *et al.* (2003). The Shank family of postsynaptic density proteins interacts with and promotes synaptic accumulation of the beta PIX guanine nucleotide exchange factor for Rac1 and Cdc42. *J. Biol. Chem.* **278**, 19220–19229.
- Audebert, S., Navarro, C., Nourry, C., Chasserot-Golaz, S., Lecine, P., Bellaiche, Y. *et al.* (2004). Mammalian Scribble forms a tight complex with the betaPIX exchange factor. *Curr. Biol.* **14**, 987–995.
- Sheng, M. & Kim, E. (2000). The Shank family of scaffold proteins. *J. Cell Sci.* **113**, 1851–1856.
- Kreienkamp, H. J. (2002). Organisation of G-protein-coupled receptor signalling complexes by scaffolding proteins. *Curr. Opin. Pharmacol.* **2**, 581–586.
- Nourry, C., Grant, S. G. & Borg, J. P. (2003). PDZ domain proteins: plug and play! *Sci. STKE*, **2003**, RE7.
- Craven, S. E. & Brecht, D. S. (1998). PDZ proteins organize synaptic signaling pathways. *Cell*, **93**, 495–498.
- Schlenker, O. & Rittinger, K. (2009). Structures of dimeric GIT1 and trimeric beta-PIX and implications for GIT-PIX complex assembly. *J. Mol. Biol.* **386**, 280–289.
- Harbury, P. B., Zhang, T., Kim, P. S. & Alber, T. (1993). A switch between two-, three-, and four-stranded coiled coils in GCN4 leucine zipper mutants. *Science*, **262**, 1401–1407.
- Im, Y. J., Lee, J. H., Park, S. H., Park, S. J., Rho, S. H., Kang, G. B. *et al.* (2003). Crystal structure of the Shank PDZ–ligand complex reveals a class I PDZ interaction and a novel PDZ–PDZ dimerization. *J. Biol. Chem.* **278**, 48099–48104.
- Appleton, B. A., Zhang, Y., Wu, P., Yin, J. P., Hunziker, W., Skelton, N. J. *et al.* (2006). Comparative structural analysis of the Erbin PDZ domain and the first PDZ domain of ZO-1. Insights into determinants of PDZ domain specificity. *J. Biol. Chem.* **281**, 22312–22320.
- Kim, S., Lee, S. H. & Park, D. (2001). Leucine zipper-mediated homodimerization of the p21-activated kinase-interacting factor, beta Pix. Implication for a role in cytoskeletal reorganization. *J. Biol. Chem.* **276**, 10581–10584.
- Paris, S., Longhi, R., Santambrogio, P. & de Curtis, I. (2003). Leucine-zipper-mediated homo- and heterodimerization of GIT family p95-ARF GTPase-activating protein, PIX-, paxillin-interacting proteins 1 and 2. *Biochem. J.* **372**, 391–398.
- Loo, T. H., Ng, Y. W., Lim, L. & Manser, E. (2004). GIT1 activates p21-activated kinase through a mechanism independent of p21 binding. *Mol. Cell. Biol.* **24**, 3849–3859.
- Botrugno, O. A., Paris, S., Za, L., Gualdoni, S., Cattaneo, A., Bachi, A. & de Curtis, I. (2006). Characterization of the endogenous GIT1–betaPIX

- complex, and identification of its association to membranes. *Eur. J. Cell Biol.* **85**, 35–46.
21. Garcia De La Torre, J., Huertas, M. L. & Carrasco, B. (2000). Calculation of hydrodynamic properties of globular proteins from their atomic-level structure. *Biophys. J.* **78**, 719–730.
 22. Terwilliger, T. C. (2003). SOLVE and RESOLVE: automated structure solution and density modification. *Methods Enzymol.* **374**, 22–37.
 23. Brunger, A. T., Adams, P. D., Clore, G. M., DeLano, W. L., Gros, P., Grosse-Kunstleve, R. W. *et al.* (1998). Crystallography & NMR System: a new software suite for macromolecular structure determination. *Acta Crystallogr. Sect. D Biol. Crystallogr.* **54**, 905–921.
 24. The CCP4 suite: programs for protein crystallography. *Acta Crystallogr. Sect. D Biol. Crystallogr.* **50** (1994), 760–763.